*J. Fluid Mech.* (1969), *vol.* 37, *part* 4, *pp.* 727–750
*Printed in Great Britain*



# Numerical integration of the three-dimensional Navier–Stokes equations for incompressible flow

By GARETH P. WILLIAMS

Geophysical Fluid Dynamics Laboratory, ESSA
Princeton University, P.O. Box 308, Princeton, New Jersey 08540

(Received 5 November 1968)

A method of numerically integrating the Navier–Stokes equations for certain three-dimensional incompressible flows is described. The technique is presented through application to the particular problem of describing thermal convection in a rotating annulus. The equations, in cylindrical polar co-ordinate form, are integrated with respect to time by a marching process, together with the solving of a Poisson equation for the pressure. A suitable form of the finite difference equations gives a computationally-stable long-term integration with reasonably faithful representation of the spatial and temporal characteristics of the flow.

Trigonometric interpolation techniques provide accurate (discretely exact) solutions to the Poisson equation. By using an auxiliary algorithm for rapid evaluation of trigonometric transforms, the proportion of computation needed to solve the Poisson equation can be reduced to less than 25% of the total time needed to advance one time step. Computing on a UNIVAC 1108 machine, the flow can be advanced one time-step in 2 sec for a $14 \times 14 \times 14$ grid upward to 96 sec for a $60 \times 34 \times 34$ grid.

As an example of the method, some features of a solution for steady wave flow in annulus convection are presented. The resemblance of this flow to the classical Eady wave is noted.

## 1. Introduction

The object of this paper is to discuss some of the problems of employing the full Navier–Stokes equations in studying viscous, incompressible, three-dimensional fluid flows. These problems are largely connected with the deduction of a stable and rational means for numerically integrating these equations. In general, it appears that there have been difficulties occurring in computational speed, stability, accuracy or treatment of boundary conditions. The particular system of equations and the domain of integration to be discussed have been designed in essence for the study of thermal convection in a rotating annulus. However, the physical considerations do not directly or crucially bear on the establishing of a stable mathematical hydrodynamic framework and the method possesses a certain generality. The method can be directly reduced to apply to (i) the Cartesian system; (ii) non-rotating flow; (iii) isothermal flow;

(iv) two-dimensional flow, or combinations of these. For more complex systems of flow only some aspects of the method are applicable.

Among the main requirements determining the design of the mathematical framework are that it should represent both the temporal and spatial distributions as faithfully as possible. Furthermore, the prediction equations should closely resemble the true Navier–Stokes equations in order that the computed flow evolution might follow that of the true fluid. It is convenient therefore to work with the basic equations in fundamental velocity–pressure form. However, it is computationally desirable to solve a Poisson equation for the pressure $p$ in order to reduce the amount of computation. The Poisson procedure filters out unimportant external gravity waves and, although it implies that the pressure adjusts instantaneously to flow changes, the assumption is not physically restrictive for the flow under consideration.

The only mathematical methods available at present for dealing with the full non-linearity and diffusivity of the Navier–Stokes equations are those using finite difference methods or finite representation by means of truncated Fourier spectra. The spatial differencing methods derived from the ideas of Arakawa (1966) have reached a level of development that provides most of the advantages of the spectral method whilst avoiding the latter's disadvantages in representing non-linear interactions and its restriction to simple geometries. Such a finite difference scheme will be presented in this paper.

In designing the finite difference equations, the well-known centred differencing is chosen for the time gradients. Such a system produces less non-physical distortion of the flow transients than do other methods, particularly some iterative methods (Kurihara 1965). We are assuming that we are interested in the time dependent part of the flow so that such distortion would be undesirable even though it could make the computation faster.

The physical aspect of the problem of annulus convection is well known and details may be obtained by consulting Williams (1967).

## 2. The continuous equations

Consider a fluid contained between two coaxial cylinders of inner and outer radii $a$, $b$ respectively and two parallel horizontal planes a distance $d$ apart (figure 1). The container rotates with respect to an inertial system at a constant rate $\boldsymbol{\Omega}$, where the rotation vector, anti-parallel to gravity $\mathbf{g}$, coincides with the axis of the cylinders. Motion is measured relative to the solid rotation in cylindrical co-ordinates $r, \phi, z$ based on the axis, $r$ being radial and $z$ vertical. The velocity components are $u$, $v$, and $w$ in the zonal, radial and vertical directions respectively.†

The fluid is thermally driven away from a state of solid rotation by an imposed horizontal temperature gradient $\Delta T$; i.e. the inner and outer cylinders are held at different constant temperatures $T_a$ and $T_b$. The base is thermally insulated and the upper surface of the fluid ($z = d$) behaves the same way owing to the presence of a lid (not in contact) inhibiting interaction with the overlying air.

† This is not standard notation.

Along with making the Boussinesq approximation, we assume for convenience that the kinematic viscosity $\nu$ and the thermometric conductivity $\kappa$ are constant and that the centrifugal acceleration is much smaller than the gravitational acceleration, i.e. $\Omega^2(a+b)/2g \ll 1$. As a consequence the upper surface can be taken to be of constant height and the free-slip rigid lid condition can be used for this surface.

The above assumptions only slightly modify the physical problem but offer convenient mathematical simplification without compromising the essential nature of the Navier–Stokes equations. Upon writing the hydrostatic pressure deviation as $\pi = p/\rho_0$, and the temperature deviation as $T$, the Navier–Stokes equations may be expressed in the following form:

$$\frac{Dv}{Dt} = -\pi_r + \nu F(v) + \left(2\Omega + \frac{u}{r}\right) u, \tag{1}$$

$$\frac{Du}{Dt} = -\frac{1}{r}\pi_\phi + \nu I(u) - \left(2\Omega + \frac{u}{r}\right) v, \tag{2}$$

$$Dw/Dt = -\pi_z + \nu H(w) + \beta g T, \tag{3}$$

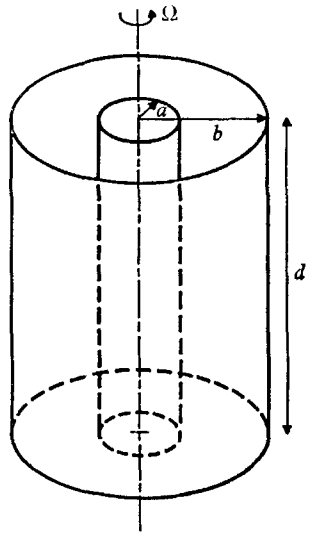


FIGURE 1. Configuration of the system for which the method is described.

with the heat transfer equation as

$$DT/Dt = \kappa \nabla^2 T, \tag{4}$$

and the equation of mass conservation as

$$(rv)_r + u_\phi + r w_z = 0, \tag{5}$$

where

$$\frac{Dq}{Dt} \equiv \frac{\partial q}{\partial t} + \frac{1}{r}(rvq)_r + \frac{1}{r}(uq)_\phi + (wq)_z, \tag{6}$$

$$F(v) \equiv \left[v_{zz} + \frac{1}{r^2} v_{\phi\phi} - w_{rz} - \frac{1}{r^2}(ru_\phi)_r\right], \tag{7}$$

$$I(u) \equiv \left[\left(\frac{1}{r}(ru)_r\right)_r + u_{zz} - \left(\frac{v_\phi}{r}\right)_r - \frac{1}{r}w_{\phi z}\right], \tag{8}$$

$$H(w) \equiv \left[\frac{1}{r}(rw_r)_r + \frac{1}{r^2}w_{\phi\phi} - \frac{1}{r}u_{z\phi} - \frac{1}{r}(rv_z)_r\right]. \tag{9}$$

In order to satisfy the continuity equation, it is convenient to derive an equation for the pressure from (1), (2) and (3). To obtain this, write the above equations of motion in convenient vector form

$$\frac{\partial \mathbf{v}}{\partial t} + \mathbf{v}.\nabla\mathbf{v} + 2\boldsymbol{\Omega} \wedge \mathbf{v} = -\nabla\pi + \beta\mathbf{g}T - \nu\nabla \wedge \boldsymbol{\omega}, \tag{10}$$

where $\boldsymbol{\omega} = \nabla \wedge \mathbf{v}$ is the vorticity and write the continuity equation in divergence $\mathscr{D}$ form

$$\mathscr{D} \equiv \nabla.\mathbf{v} = -\frac{1}{\rho}\frac{D\rho}{Dt} = 0. \tag{11}$$

The divergence of (10)

$$(\partial\mathscr{D}/\partial t) = -[\nabla^2\pi - \beta g T_z - 2\boldsymbol{\Omega}\boldsymbol{\omega} + \nabla.(\mathbf{v}.\nabla\mathbf{v})], \tag{12}$$

is an equation for the prediction of $\mathscr{D}$. To maintain the incompressible continuity $\mathscr{D} \equiv 0$, $\pi$ must satisfy the right member of (12) set to zero. This condition can be expressed as

$$\nabla^2\pi = \nabla.\mathbf{G}, \tag{13}$$

where $\mathbf{G}$ are the components (inertia terms, etc.) of the prediction equations. The boundary conditions for (13) are that

$$\pi_n = G^n; \tag{14}$$

i.e. the normal pressure gradients must equal the component terms of the normal velocity equation on each boundary. The index $n$ represents the variables $r$ or $z$. In the $\phi$-direction the condition is that the flow be periodic.

Equation (13) is of an elliptic type, denoted say as

$$\mathscr{L}(\pi) = Q, \tag{15}$$

and is subject to inhomogeneous Neumann boundary conditions which we denote as

$$\mathscr{M}(\pi) = BC,$$

where $\mathscr{L}$ and $\mathscr{M}$ are linear differential operators. The principle behind solving such a system is to reduce the problem to one with homogeneous boundary conditions (see e.g. Lanczos 1961, p. 435). To do this let $\pi_0$ be any reasonable function satisfying the boundary conditions. Then $\pi^* = \pi - \pi_0$ satisfies a linear boundary value problem with homogeneous boundary conditions, i.e.

$$\mathscr{L}[\pi^*] = Q^* \equiv Q - \mathscr{L}[\pi_0], \tag{16}$$

in the interior with $\mathscr{M}[\pi^*] = 0$ on the boundary. A Poisson equation of this type can be reduced to an ordinary second-order differential equation by expanding the variables in eigenfunctions. It will be seen later that this feature of the continuous Poisson equation has a most useful analogy in the finite difference formulation.

## 3. The grid system

To turn the above equations into a practical scheme of computation, they are expressed in finite difference form on the following grid arrangement. The pressure and temperature variables which are defined at the same points form the basic grid. The velocity components $u$, $v$, $w$ are all defined at different points interlacing with the basic grid.

In a horizontal cross-section the $\pi$, $T$ points are distributed around radial circles. The zonal velocity points lie on the same circles midway between the $\pi$ points (figure 2). Radial velocity points lie along radii through the $\pi$ points and are located midway between the $\pi$ points. Finally, $w$ points lie on the vertical lines of the $\pi$ grid, midway between points (figure 3). The physical boundaries are placed so that they fall halfway between the two extreme $\pi$ points.

The continuous co-ordinates $(r, \phi, z)$ are thus replaced by the discrete grid system $(I, J, K)$ such that

$$\left.\begin{aligned} r &= a+(I-\tfrac{3}{2})\,\Delta r \quad (I = 1,2,\ldots,L+1);\\ \phi &= (J-1)\,\Delta\phi \quad\;\; (J = 1,2,\ldots,M+1);\\ z &= (K-\tfrac{3}{2})\,\Delta z \quad (K = 1,2,\ldots,N+1) \end{aligned}\right\} \tag{17}$$

give the co-ordinates of the $\pi$ points. The grid lengths between $\pi$ points are given by

$$\Delta r = (b-a)/(L-1), \quad \Delta\phi = \Phi/(M-1), \quad \Delta z = d/(N-1). \tag{18}$$

The angular size of the annulus $\Phi$ is normally $2\pi$ but the formulation will treat the general case by assuming periodicity. The interlacing grids of the velocity points can be similarly indexed.

The interlaced grid system presents little problem in establishing the finite difference equations and appears to be over-all the most consistent arrangement. The discrete fluid element centred on $\pi$ and bounded by the $u$, $v$, $w$ points forms the fundamental fluid element for which most concepts and properties such as mass conservation apply. The grid system as a whole is uniform and symmetric as far as point arrangement goes, i.e. there is no preferred direction. There is of course a geometrical variation.

## 4. The finite difference equations

Having divided the fluid into small elements by a series of grid points which are spaced at distances of $\Delta r$, $\Delta z$ and $r\Delta\phi$, the time variable is next split up into increments of $\Delta t$ such that $t = \tau.\Delta t$ where $\tau$ denotes the current time-index. To exhibit the finite difference equations and their multi-dimensional properties in compact form, we define the following difference and averaging operators in the notation of Richardson (1922) and Shuman (1962),

$$\left.\begin{aligned} \delta_x q &\equiv [q(x+\tfrac{1}{2}\Delta x)-q(x-\tfrac{1}{2}\Delta x)]/\Delta x,\\ \bar{q}^x &\equiv [q(x+\tfrac{1}{2}\Delta x)+q(x-\tfrac{1}{2}\Delta x)]/2, \end{aligned}\right\} \tag{19}$$

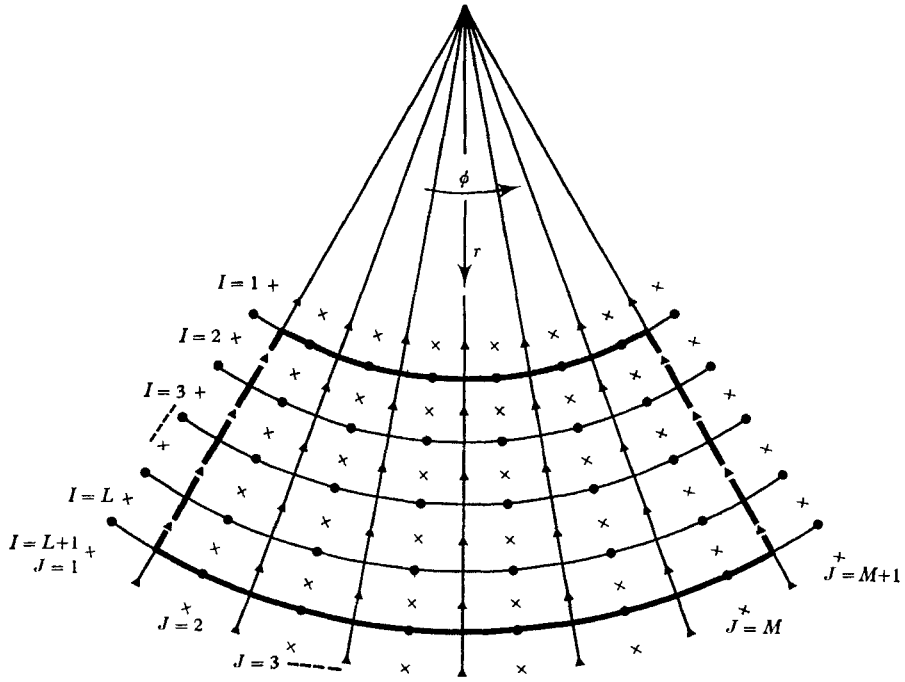


FIGURE 2. Grid arrangement in the horizontal. $\pi$, $T$ points are the centre of basic fluid elements. Broken lines indicate the periodic boundaries and heavy lines denote cylinder walls. ×, pressure, temperature point; ●, radial velocity point; ▲, zonal velocity point.

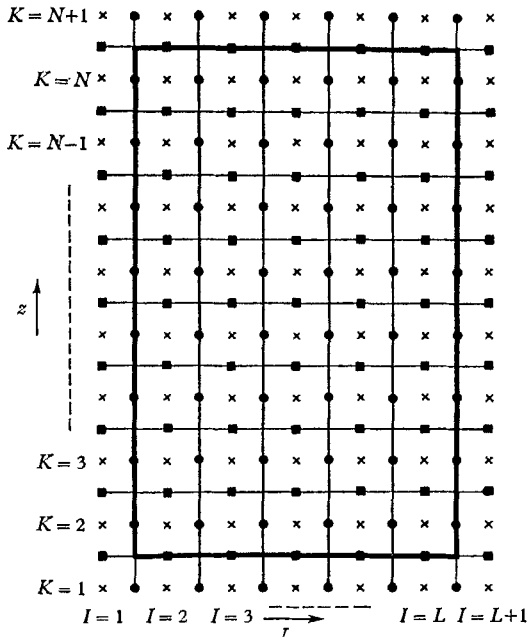


FIGURE 3. Grid arrangement in the vertical. ×, pressure, temperature point; ●, radial velocity point; ■, vertical velocity point.

where $q$ represents one of the field variables, $x$ ($\equiv r, \phi, z, t$) one of the co-ordinates and $\Delta x$ is the discrete grid interval of $x$. The bar and delta operators form a linear commutative and distributive algebra for which various operator rules and identities can be constructed, e.g.

$$\delta_x(q_1 q_2) = \bar{q}_1^x \delta_x q_2 + \bar{q}_2^x \delta_x q_1.$$

For further examples and applications the fundamental paper on numerical methods by Lilly (1964) should be consulted.

In this notation, a set of finite difference equations can be established in the following form:

$$\delta_t \bar{v}^t + \frac{1}{r}\delta_r(\overline{rv}^r . \bar{v}^r) + \frac{1}{r}\delta_\phi(\bar{u}^r . \bar{v}^\phi) + \delta_z(\bar{w}^r . \bar{v}^z) = -\delta_r \pi + \nu F^*(v) + \overline{(2\Omega u + \{u^2/r\})}^{r\phi}, \quad (20)$$

$$\delta_t \bar{u}^t + \frac{1}{r}\delta_r(\overline{rv}^\phi . \bar{u}^r) + \frac{1}{r}\delta_\phi(\bar{u}^\phi . \bar{u}^\phi) + \delta_z(\bar{w}^\phi . \bar{u}^z) = -\frac{1}{r}\delta_\phi \pi + \nu I^*(u) - \left(2\Omega + \frac{u}{r}\right)\frac{1}{r}\overline{(rv)}^{r\phi}, \quad (21)$$

$$\delta_t \bar{w}^t + \frac{1}{r}\delta_r(\overline{rv}^z . \bar{w}^r) + \frac{1}{r}\delta_\phi(\bar{u}^z . \bar{w}^\phi) + \delta_z(\bar{w}^z . \bar{w}^z) = -\delta_z \pi + \nu H^*(w) + \beta g \bar{T}^z, \quad (22)$$

$$\delta_t \bar{T}^t + \frac{1}{r}\delta_r(rv\bar{T}^r) + \frac{1}{r}\delta_\phi(u\bar{T}^\phi) + \delta_z(w\bar{T}^z) = \kappa\left[\frac{1}{r}\delta_r(r\delta_r T) + \frac{1}{r^2}\delta_{\phi\phi}T + \delta_{zz}T\right]_{\text{lag}}, \quad (23)$$

$$\delta_r(rv) + \delta_\phi u + r\delta_z w \equiv 0, \quad (24)$$

where

$$\left.\begin{aligned} F^*(v) &\equiv \left[\delta_{zz}v + \frac{1}{r^2}\delta_{\phi\phi}v - \delta_{rz}w - \frac{1}{r^2}\delta_r(r\delta_\phi u)\right]_{\text{lag}}, \\ I^*(u) &\equiv \left[\delta_r\left(\frac{1}{r}\delta_r(ru)\right) + \delta_{zz}u - \delta_{r\phi}\left(\frac{v}{r}\right) - \frac{1}{r}\delta_{z\phi}w\right]_{\text{lag}}, \\ H^*(w) &\equiv \left[\frac{1}{r}\delta_r(r\delta_r w) + \frac{1}{r^2}\delta_{\phi\phi}w - \frac{1}{r}\delta_{z\phi}u - \frac{1}{r}\delta_{rz}(rv)\right]_{\text{lag}}. \end{aligned}\right\} \quad (25)$$

These expressions and operator notation must be interpreted with respect to the grid-point of the variable under consideration. The centred time differencing is for the level $\tau$ so that the predictions yield the variables at level $(\tau+1)$. The non-linear, rotational and pressure terms are evaluated at the central level $\tau$ whereas the diffusive terms use the non-central $(\tau-1)$ level, denoted by the subscript 'lag'. The continuity equation (24) applies at a $\pi$ point and is valid for the fluid unit surrounding that point. The averaging in the equations is necessary to provide variable values at grid points where the variables are not explicitly defined, e.g. in the buoyancy term, $\bar{T}^z$ averages two neighbouring $T$ values to give their mean as the value at an intermediate point which happens to be the $w$ point being predicted. Through using an interlacing grid system the amount of averaging of this type is reduced to a minimum thus improving accuracy. Furthermore, the continuity equation has a unique exact form which can only be achieved by such a grid; this uniqueness is essential for deriving the Poisson equation. The only disadvantage occurs in the rotational terms, where products

such as $uv$ must be averaged as $u$ and $v$ occur at different locations. Defining $\pi$ and $T$ at the same point is desirable for consistency with the equation of state

$$\rho = \rho_0[1-\beta T].$$

The variables $u$, $v$, $w$ and $T$ may be obtained by marching equations (20)–(23). To obtain $\pi$ and satisfy continuity, a Poisson equation must be derived. To achieve this, suppose for convenience that the prediction equations can be written as

$$\left.\begin{aligned} \delta_t \bar{v}^t &= -\delta_r \pi + GV, \\ \delta_t \bar{u}^t &= -(1/r)\,\delta_\phi \pi + GU, \\ \delta_t \bar{w}^t &= -\delta_z \pi + GW, \end{aligned}\right\} \tag{26}$$

where $\mathbf{G} \equiv (GV, GU, GW)$ represents the non-linear, viscous and rotational terms. Substituting these equations into the continuity equation (24) gives

$$\nabla^2 \pi = \nabla . \mathbf{G}, \tag{27}$$

where

$$\nabla^2 \pi \equiv \frac{1}{r}\delta_r(r\delta_r \pi) + \frac{1}{r^2}\delta_{\phi\phi}\pi + \delta_{zz}\pi,$$

and

$$\nabla . \mathbf{G} \equiv \frac{1}{r}\delta_r(rGV) + \frac{1}{r}\delta_\phi GU + \delta_z GW. \tag{28}$$

Solving (27) during each time-step provides the values of $\pi$ needed to complete the marching process. (See § 5*b* for minor modification.)

In executing the calculation the components of $\mathbf{G}$, (26), can be evaluated from the variables of the previous time step. Forming the divergence of $\mathbf{G}$,† the Poisson equation (27) on solution gives values of $\pi$. Using these values of $\mathbf{G}$ and $\pi$, the variables $u$, $v$, $w$ and $T$ at the next time step can then be directly evaluated. The use of the same numerical values of $\mathbf{G}$ in the Poisson and prediction equations guarantees consistency and satisfaction of the integral constraint (§ 6*e*) for the existence of the solution. The boundary conditions then yield the external values of the variables.

Reasons for preferring the above finite difference forms (mainly because of stability requirements) and other detailed features of the numerical scheme will be discussed in the next section.

## 5. Remarks concerning the finite differencing

In this section we will examine the different types of computational instability inherent in finite difference forms of the Navier–Stokes equations and how they can be neutralized by the chosen system.

### (*a*) *Instability of the convection terms*

Consider an equation representative of the convection process:

$$\delta_t \bar{q}^t + q\delta_x \bar{q}^x = 0. \tag{29}$$

The linearized form

$$\delta_t \bar{q}^t + q_0 \delta_x \bar{q}^x = 0, \tag{30}$$

† This must be done numerically from previously calculated $\mathbf{G}$ values and not by differencing the individual terms of each component and calculating those.

has a well known partial instability (for instance, Richtmyer 1957) which can be suppressed by realizing the Courant–Friedrichs–Lewy criterion that the time-step increment be limited to $\Delta t \leqslant \Delta x/|q_0|$.

The Courant–Friedrichs–Lewy criterion alone does not suffice for the integration of the non-linear equation (29) and the computation eventually becomes unstable. The instability arises after numerous time-steps when the appearance of large truncation errors causes an almost explosive increase in the total energy of the system. Phillips (1959) has shown that uncontrolled *aliasing* (Blackman & Tukey 1958) causes this instability. Aliasing happens when waves that are too short to be resolved by a given set of grid points are misrepresented by long waves (Hamming 1962). The convection term can produce this phenomenon because the non-linear interactions combine certain frequencies to produce higher frequencies which lie outside the limit of resolution set by the grid. Thus non-linear instability or quasi-non-linear instability (Miyakoda 1962) has its origin in space truncation errors.

However, Arakawa (1966) has shown that it is possible to devise forms of the convection terms for which non-linear computational instability does not occur because the aliasing is controlled. If the convection terms are written in the total derivative form

$$\delta_x(\bar{q}^x . \bar{q}^x),$$

as they are in equations (20)–(23), some of the integral constraints on quantities of physical importance, such as conservation of kinetic energy and the quadratic quantities $u^2$, $v^2$, $w^2$ and $T^2$ can be maintained for the finite difference forms $(\overline{u^2})^\phi$, $(\overline{w^2})^z$, $(1/r)\,(\overline{rv^2})^r$ and $T^2$. In this situation non-linear instability can not occur. This follows from the fact that, if the square of a quantity is conserved when summed over all grid points in a domain, the quantity itself will be bounded at every grid point for the entire integration period. Aliasing can still exist in the stable conserving scheme, appearing perhaps as a phase error or as a distortion of the energy spectrum. However, the total energy and thence the average scale of the motion are free from aliasing errors.

In summary, the stability of the convection terms can be ensured by (i) meeting the Courant–Friedrichs–Lewy criterion† and (ii) by expressing the finite difference formulation in total derivative form to guarantee its satisfaction of the equivalent to Gauss's divergence theorem (see Bryan 1966) and the consequent conservation of a variable and its quadratic.

### (*b*) *Weak instability of time differencing*

Whereas the above instability is due to the convection term, the instability of this section is due to the prediction term. An equation such as

$$\delta_t \bar{q}^t + \delta_x(\bar{q}^x . \bar{q}^x) = 0, \tag{31}$$

involves variables at three time levels, which indicates that the first-order continuous equation has been raised to a second-order difference equation. This introduces a non-physical computational mode into the solution (Platzman 1958). The mode takes the form of an oscillation, with respect to time, about the

† Where $q_0$ now represents the maximum possible $q$.

true solution. The amplitude of the oscillation grows slowly with time and eventually leads to the formation of two separate solutions at the even and odd time steps. Hence the resulting instability is referred to as 'time splitting' (Henrici 1962).

Integrations of an equation similar to (31) over a long period of time show that the solutions correspond very accurately to their analytical counterparts provided the instability remains small (Lilly 1965). Furthermore, the kinetic energy values indicate that time splitting occurs and can amplify considerably before the average kinetic energy deviates from a constant value. After several hundred time steps the instability dominates the solution and the kinetic energy deviation arises.

On the other hand, a study of methods other than the central time differencing displayed an undesirably strong damping of the kinetic energy (Kurihara 1965). Thus the central differencing method is preferable provided the weak instability can be controlled. This can be done simply by periodically averaging the variables over adjacent time steps (Arakawa 1965, private communication) and restarting the calculation with the averaged values. The computational mode is not eliminated but is suppressed.

The continuity divergence variable $\mathscr{D}$ exhibits an instability of a type similar to that described above for the velocity and temperature variables. If the Poisson equation (27) can be solved exactly, there is no problem. In reality, however, a degree of round-off error is inevitable even with the trigonometric method. This in turn creates an artificial divergence which can lead to computational instability. A similar behaviour was noted by Smagorinsky (1958) in a comparable computational system devised and rejected for integrations for the general circulation of the atmosphere.

It was found that this computational difficulty can be overcome by using a computational strategem; the round-off divergence at one step is used as a correction term in the forcing terms of the Poisson equation. Thus instead of (27) we take the original divergence equation, i.e.

$$\nabla^2\pi = \nabla . \mathbf{G} - \delta_t \overline{\mathscr{D}}^t. \tag{32}$$

Since the divergence in the computation at a given step $(\tau - 1)$ is not exactly zero $(\mathscr{D}^{\tau-1} \neq 0)$ but that at $(\tau + 1)$ ought to be zero $(\mathscr{D}^{\tau+1} = 0)$, (32) is written

$$\nabla^2\pi = \nabla . \mathbf{G} + (\mathscr{D}^{\tau-1}/2\Delta t). \tag{33}$$

By solving this form of the equation and repeating the process of inserting the round-off error into the forcing function it is found that $\mathscr{D}$ does not grow and remains bounded at the order of the round-off errors. Harlow & Welch (1965) introduced this technique of controlling $\mathscr{D}$ for the case of two-dimensional flow in which relaxation procedures are used to solve the Poisson equation.

A computation with $\mathscr{D}^{\tau}$ instead of $\mathscr{D}^{\tau-1}$ in (33) gives unstable $\mathscr{D}$ growth, indicating the sensitivity of the stability requirement. The growth of $\mathscr{D}$ in forms of the Poisson equation other than (33) is most likely due to the centred time differencing and the associated presence of a weak instability of the 'splitting' variety.

### (*c*) *Instability of the diffusion terms*

The diffusive terms in the prediction equations have a well-known strong partial instability (for instance Richtmyer 1957). This can be suppressed by limiting the time step to $\Delta t < (\Delta x)^2/8\nu$, $\Delta t < (\Delta x)^2/8\kappa$ whichever is the lesser.

### (*d*) *Formulating the friction terms*

If the conventional form of the friction terms, i.e. $\nu\nabla^2\mathbf{v}$ had been used in the equations leading to the formulation of the Poisson equation (32), then the friction terms would have made a round-off contribution of $\nu\nabla^2\mathscr{D}$ to the forcing function. To avoid this feature in the finite difference system the friction terms must be expressed directly in terms of the vorticity, i.e. as $\nu\mathbf{F} = -\nu\nabla\wedge\boldsymbol{\omega}$. In terms of components this is expressed as

$$\left.\begin{aligned} F^*(v) &= \delta_z\eta - (1/r)\,\delta_\phi\zeta, \\ I^*(u) &= \delta_r\zeta - \delta_z\xi, \\ H^*(w) &= (1/r)\,\delta_\phi\xi - (1/r)\,\delta_r(r\eta), \end{aligned}\right\} \tag{34}$$

where $$\xi = (1/r)\,\delta_\phi w - \delta_z u, \quad \eta = \delta_z v - \delta_r w, \quad \zeta = (1/r)\,\delta_r(ru) - (1/r)\,\delta_\phi v. \tag{35}$$

Substituting (35) into (34) yields the expressions of (25). Furthermore, from (34) it follows that $\nabla\mathbf{F}$, the contribution to the Poisson equation, is identically zero. If formulations other than that using the vorticity definition are used, this identity does not hold because of truncation problems in differencing geometrical factors.

The vorticity formulation also provides a convenient form of the boundary condition on the normal pressure gradient. In this condition the friction must be evaluated at the boundary and, whereas in the standard formulation this would involve variable values at $-\Delta x$ outside the boundary, the vorticity method involves values at only $-\frac{1}{2}\Delta x$ outside. This improves accuracy.

### (*e*) *Formulating the rotation terms*

The finite difference formulations of the rotation terms in the $v$, $u$ equations (20), (21) are interrelated because of the need to maintain a zero net contribution from them to the kinetic energy. However, some arbitrariness exists in the way the rotational terms can be set up because of the need to average variables on the interlaced grid system. It can be shown, by algebraic manipulation (for an example of which see Lilly 1964), that the forms of (20) and (21) have the desired property of conserving kinetic energy and angular momentum. The rotation term in the $v$ equation is essentially a single term originating in the kinematical acceleration $(r\Omega + u)^2$, (with the $\Omega^2$ part neglected), and has been treated as such.

### (*f*) *The boundary conditions*

The boundary conditions express the state of the fluid at the boundaries. Computationally these conditions when expressed in finite difference form must provide definitions of the variables at the boundaries or at points just outside

the boundaries† and must also maintain the finite difference properties such as energy conservation for the fluid near the boundary. The external values are needed for evaluation of the prediction components **G**, (26), at points adjacent to the boundary. For a staggered grid, the simplest and most obvious form for the boundary conditions also appears to be the best for conservation and consistency.

Thus in annulus convection, for example, the conditions are as follows: (i) the base is an insulated non-slip surface for which a suitable form for the boundary conditions is

$$\left.\begin{aligned} w = \bar{v}^z = \bar{u}^z = \delta_z T = 0, \\ \delta_z \pi = \beta g \bar{T}^z + \nu \left[ -\frac{1}{r}\delta_{z\phi} u - \frac{1}{r}\delta_{rz}(rv) \right], \end{aligned} \right\} \tag{36}$$

applied at $z = 0$; (ii) the upper fluid surface is an insulated free slip surface with conditions

$$\left.\begin{aligned} w = \delta_z u = \delta_z v = \delta_z T = 0, \\ \delta_z \pi = \beta g \bar{T}^z, \end{aligned} \right\} \tag{37}$$

applied at $z = d$; (iii) on the non-slip sidewalls, the conditions are

$$v = \bar{w}^r = \bar{u}^r = 0,$$

$$\delta_r \pi = \nu \left[ -\delta_{rz} w - \frac{1}{r^2}\delta_r(r\delta_\phi u) \right],$$

and $\bar{T}^r = T_a, T_b$ applied at $r = a, b$ respectively.

### (g) *Truncation errors*

Truncation errors of the prediction equations are of order $(\Delta x)^2$ or $(\Delta t)^2$.

## 6. Details of the Poisson solution

The general principle behind solving an elliptic equation (15) with inhomogeneous Neumann boundary conditions was discussed earlier. The details of solving the particular finite difference equation (27) rapidly will be presented in this section.

(*a*) The first step in solving equation (33) which we write as $\nabla^2 \pi = Q$, is to find a function $\pi_0$ which satisfies the boundary conditions $\delta_n \pi = BC$. One such function can be formed by setting $\pi_0 = 0$ at all interior pressure points and setting $\pi_0 = \pm BC.\Delta n$ at points outside the boundary. The formation of $\nabla^2 \pi_0$ for modifying $Q$ is restricted to points lying just inside the boundary at which $Q^* = Q \mp BC/\Delta n$‡ while in the remainder of the interior $Q^* = Q$ holds. The problem is then to solve $\nabla^2 \pi^* = Q^*$ with $\delta_n \pi^* = 0$ where $\pi^* = \pi - \pi_0$ and $Q^* = Q - \nabla^2 \pi_0$.

† External points are a computational device to introduce the boundary conditions and to avoid having to redefine the finite difference equations near the boundaries.

‡ With minor modification factors at $r = a, b$.

(*b*) The boundary conditions on $\pi^*$ are met by expanding $\pi^*$ in a finite eigenfunction series. In the $\phi$-direction, a periodic trigonometric expansion suits the periodic boundary conditions whereas for the vertical direction cosine expansion suits the condition of a zero pressure gradient. Thus we expand $\pi^*$ into two series of harmonics (rather than into a single series of double harmonics, which is computationally slower)

$$\pi^* = \sum_{\alpha=0}^{M-2} P_\alpha H_\alpha(J),$$

$$P_\alpha = \sum_{\beta=0}^{N-2} P_{\alpha\beta} H_\beta(K), \tag{38}$$

where $\alpha$, $\beta$ are indices for the periodic and cosine coefficients respectively. The eigenfunctions are

$$\left.\begin{aligned} H_\alpha(J) &\equiv \Gamma_\alpha \cdot \left(\frac{2}{M-1}\right)^{\frac{1}{2}} \cdot \cos\left(\frac{2\pi\alpha}{M-1} \cdot (J-1)\right) \quad \text{for} \quad \alpha = 0, 1, 2, \ldots, \tfrac{1}{2}(M-1), \\ H_\alpha(J) &\equiv \left(\frac{2}{M-1}\right)^{\frac{1}{2}} \cdot \sin\left\{\frac{2\pi}{M-1}(J-1)\left(\alpha - \frac{M-1}{2}\right)\right\} \quad \text{for} \quad \alpha = \tfrac{1}{2}(M-1)+1, \ldots, M-2, \end{aligned}\right\} \tag{39}$$

where $J = 1, 2, \ldots, M$ and $\Gamma_\alpha = 2^{-\frac{1}{2}}$ for $\alpha = 0$ and $\alpha = \frac{1}{2}(M-1)$† but $\Gamma_\alpha = 1$ for other $\alpha$. Also

$$H_\beta(K) \equiv \Gamma_\beta \left(\frac{2}{N-1}\right)^{\frac{1}{2}} \cos\left(\frac{\pi}{N-1}\beta(K-\tfrac{3}{2})\right) \quad \text{for} \quad \beta = 0, 1, 2, \ldots, N-2, \tag{40}$$

where $K = 2, 3, \ldots, N$. $\Gamma_\beta = 2^{-\frac{1}{2}}$ when $\beta = 0$ but is otherwise equal to unity. This non-standard cosine expansion allows for boundaries that lie between grid points; $H_\beta(K=1) = H_\beta(K=2)$ so that $\delta_z H_\beta = 0$ at $z = 0$ reflects this. The number of coefficients in each series equals the number of grid points in the corresponding direction so each series uniquely matches the data (see e.g. Lanczos 1961, p. 89).

Expanding $\pi^*$ and $Q^*$ in series and substituting into (27) gives a second-order difference equation for the coefficients:

$$(1/r)\,\delta_r(r\delta_r P_{\alpha\beta}) - \{\lambda_\beta + (\lambda_\alpha/r^2)\} P_{\alpha\beta} = Q_{\alpha\beta}, \tag{41}$$

where

$$\lambda_\alpha = \frac{2}{(\Delta\phi)^2}\left(1 - \cos\frac{2\pi\alpha}{M-1}\right) \quad \text{for} \quad \alpha = 0, 1, \ldots, \tfrac{1}{2}(M-1),$$

$$\lambda_\alpha = \frac{2}{(\Delta\phi)^2}\left\{1 - \cos\frac{2\pi}{M-1}\left(\alpha - \frac{M-1}{2}\right)\right\} \quad \text{for} \quad \alpha = \tfrac{1}{2}(M-1)+1, \ldots, M-2,$$

$$\lambda_\beta = \frac{2}{(\Delta z)^2}\left(1 - \cos\frac{\beta\pi}{N-1}\right) \quad \text{for} \quad \beta = 0, 1, \ldots, N-2.$$

(*c*) To solve the ordinary difference equation (41) subject to the boundary conditions $\delta_r P_{\alpha\beta} = 0$, it is written out in full as

$$-A_I(P_{\alpha\beta})_{I+1} + B_I(P_{\alpha\beta})_I - C_I(P_{\alpha\beta})_{I-1} = D_I, \tag{42}$$

† $M$ is restricted to odd integers.

where
$$A_I = 1,$$
$$B_I = [2r + (\Delta r)^2 (r^{-1}\lambda_\alpha + r\lambda_\beta)]/[r + \Delta r/2],$$
$$C_I = [r - \Delta r/2]/[r + \Delta r/2],$$
$$D_I = -[(r(\Delta r)^2)/(r + \Delta r/2)]\,(Q_{\alpha\beta})_I.$$

The boundary conditions are $(P_{\alpha\beta})_{I=1} = (P_{\alpha\beta})_{I=2}$,

and
$$(P_{\alpha\beta})_{I=L+1} = (P_{\alpha\beta})_{I=L}.$$

(*d*) To avoid exponential solutions in solving (41) the recursion functions $E_I$, $F_I$ are introduced by
$$(P_{\alpha\beta})_I = (P_{\alpha\beta})_{I+1} E_I + F_I, \tag{43}$$
with $E_1 = 1$, $F_1 = 0$ (for instance, Richtmyer 1957). Substituting into (42) gives
$$E_I = 1/(B_I - C_I E_{I-1}), \quad F_I = E_I(D_I + C_I F_{I-1})$$
which can be calculated for $I = 1$ to $I = L$ ($E_I$ is a fixed function and need only be calculated once). The boundary condition gives $(P_{\alpha\beta})_{L+1} = F_L/(1 - E_L)$ and thence all $P_{\alpha\beta}$ may be calculated for $I = L, L-1, L-2, \ldots$, downward to 1 using (43) and the known $E_I$, $F_I$.

(*e*) When $\alpha = \beta = 0$, then $\lambda_\alpha = \lambda_\beta = 0$ and the above recursion scheme no longer works. Equation (41) reduces to $(1/r)\,\delta_r(r\delta_r P_{00}) = Q_{00}$ and the conditions $\delta_r P_{00} = 0$ on $r = a, b$ make it degenerate. A study of this degenerate mode reveals the nature of this type of Poisson equation and the constraints that are necessary for solutions to exist. This equation has a solution provided
$$\sum_{I=2}^{L} Q_{00} r\,\Delta r = 0. \tag{44}$$

To prove that this holds we recollect that $Q \equiv \nabla . \mathbf{G}$ and $\delta_n \pi = G^n$; thence $Q^* = \nabla . \mathbf{G}^*$, where $\mathbf{G}^* = \mathbf{G} - \nabla \pi_0$ is zero on the boundaries. Thus
$$\sum_{I=2}^{L} Q^* = \sum_{I=2}^{L} \nabla . \mathbf{G}^* = 0$$
indicates the veracity of (44). This constraint is also a reflexion of Gauss's theorem, i.e. in the continuous
$$\int \nabla^2 \pi \, d\tau = \int \nabla \pi . d\mathbf{s}; \quad \int Q \, d\tau = \int \mathbf{G} . d\mathbf{s},$$
so that
$$\int (\nabla^2 \pi - \nabla \mathbf{G})\, d\tau = \int (\nabla \pi - \mathbf{G}) . d\mathbf{s} = 0.$$

The boundary condition on the normal pressure gradient must therefore be consistent with the basic equations; in finite difference form $Q$ must be formed from the components of the prediction equations. This places a constraint (44) on the finite difference formulation. The constraint arises only in the zero–zero

coefficient because it is identically satisfied by the trigonometric functions $H_\alpha$, $H_\beta$ in the non-zero modes. The actual solution of $P_{00}$ can be obtained by a direct marching of the equation, with the upper boundary condition being met implicitly by virtue of (44). The absolute value of $P_{00}$ is undefined as a consequence of the fact that $\pi$ can only be determined to within an arbitrary constant.

(*f*) Trigonometric synthesis of the $P_{\alpha\beta}$ yields the pressure $\pi^*$. In the actual computation the only trigonometric transforms performed are this synthesis, equation (38), and the analysis of the forcing function $Q^*$, i.e.

$$\left.\begin{aligned} Q_\alpha &= \sum_{J=1}^{M-1} Q^* H_\alpha(J), \\ Q_{\alpha\beta} &= \sum_{K=2}^{N} Q_\alpha H_\beta(K). \end{aligned}\right\} \tag{45}$$

(*g*) A method for performing the trigonometric transforms (38) and (45) in a rapid fashion by reducing the amount of multiplication in these summations is given in the appendix. This is achieved by taking advantage of the symmetry properties of the trigonometric functions. By this device the time needed to solve the Poisson equation can be reduced so that it occupies less than $\frac{1}{4}$ of the computational time.

(*h*) We note in passing that in our choice of eigenfunctions we avoided using the Bessel functions associated with the radial co-ordinate. Although this choice is arbitrary the use of the $E$, $F$ recursion scheme in the $r$-direction is computationally advantageous compared with using Bessel functions.

## 7. Integral properties

An apparent simulation of physically observed characteristics does not in itself form an understanding of the flow. Diagnostic integral techniques provide a very sensitive measure of the mechanical similarity of model to physical entity and together with an analysis of component terms (Williams 1967) could provide the type of insight from numerical studies that is normally derived from analytical studies.† For, although numerical methods are capable of accounting for non-linearity and other complexities, they do not yield an immediate understanding of the mechanics involved. However, in the integrated form of the equations the non-linear effects vanish or are simplified and this makes the task of their interpretation easier than that of the full prediction equations. The balancing of the energy components also provides some confirmation of a proper execution of the computation. The use of different integral expressions for describing the mechanics has been an important technique developed in recent years for numerical solutions in meteorology (see e.g. Smagorinsky, Manabe & Holloway 1965). The type of integral that is of use in analyzing a solution varies from problem to problem.

The simplest integrals that are useful diagnostic and interpretative tools are

† It is to be emphasized that this paper deals only with how numerical solutions may be obtained. It is equally important to develop methods of analyzing the solutions.

the total or global integrals for kinetic and potential energy; in the continuous form these are respectively:

$$E_K = \langle \tfrac{1}{2}(u^2+v^2+w^2)\rangle, \quad E_P = \langle -\beta g z T\rangle,$$

where

$$\langle(\ )\rangle \equiv \int_a^b r\,dr \int_0^{\Phi} d\phi \int_0^d dz\,(\ ).$$

Defining conversion and diffusion integrals as

$$E_K : E_P = \beta g \langle wT\rangle,$$
$$\epsilon_K = \nu \langle vF(v) + uI(u) + wH(w)\rangle,$$
$$\epsilon_P = -\beta g \kappa \langle z \nabla^2 T\rangle,$$

the integrated forms of the prediction equations (1) to (4) are

$$(E_K)_t = E_K : E_P + \epsilon_K,$$
$$(E_P)_t = -E_K : E_P + \epsilon_P.$$

It is only a question of lengthy algebra to show that the finite difference equations also yield discrete energy summations and equations of the same form. The use of the conserving form for the convection terms ensures this and that the conversion rates of potential and kinetic energies are equal.

## 8. Results

The veracity and feasibility of the computational method lies in the demonstration of its practicality. Most numerical studies of this type are limited or compromised by the amount of information that the computer can handle. The method has been programmed for a UNIVAC 1108 computer.† When the program utilizes only the immediately available core storage the computation is rapid (less than 2 sec per time step) but is limited in resolution to a maximum of $(14)^3$ points. For higher resolution it is necessary to use limited access drums for temporary allocation of the variables and the programming becomes highly complex. The program is set up so that during the marching of the variables only three $(\phi, z)$ planes of the variables need be placed in core storage at a given time, the remainder being held on the drums. By using drums with a storage capacity of approximately 1·4 million words and a core storage of approximately 50,000 words, resolutions of up to $60 \times 34 \times 34$ can be considered.

In table 1 the computation times per step for different resolutions are shown. The maximum time is 96 sec and although calculations with such a resolution are time-consuming it does represent an upper bound for the method; a bound which can be reduced with advances in technology or improvements in programming. Comparing the low resolution all-core storage program with the drum storage method at a $(14)^3$ resolution, the drum method requires 0·77 sec longer because of the drum transfers. This inefficiency is less at higher resolutions. The Poisson section occupies only 16 % of the computation time in the core formulation but about 23 % in the drum formulation, for all resolutions.

† A comparative calculation using this method and the method described in Williams (1967) produced similar results.

The method discussed above is being used to study annulus convection and other fluid dynamical systems. As such solutions and their analysis are of an extensive nature, the physical aspect of the solutions will be presented separately in a forthcoming paper.

In figure 4 we present merely an outline of a solution for the so-called steady wave flow of the Rossby régime of annulus convection. Starting from an initial condition of isothermal solid rotation, integration to a steady state was made. The configuration parameters are $a = 2\,\text{cm}$, $b = 5\,\text{cm}$, $d = 3\,\text{cm}$, $\Delta T = 5\,^{\circ}\text{C}$, $\Omega = 0{\cdot}8\,\text{rad}\,\text{sec}^{-1}$ and the physical parameters for water at $20\,^{\circ}\text{C}$ are

| Resolution | | | Time per time step (sec) | Time on Poisson sect. (sec) | Percentage on Poisson | Method of storage |
|---|---|---|---|---|---|---|
| $L+1$ | $M+1$ | $N+1$ | | | | |
| 14 | 14 | 14 | 2·00 | 0·32 | 16 | Core |
| 14 | 14 | 14 | 2·77 | 0·63 | 23 | Drum |
| 14 | 42 | 14 | 7·70 | 1·80 | 23 | Drum |
| 22 | 22 | 22 | 11·4 | 2·59 | 23 | Drum |
| 34 | 34 | 34 | 51·7 | 12·4 | 24 | Drum |
| 60 | 34 | 34 | 95·7 | 22·7 | 24 | Drum |
| 38 | 38 | 34 | 66·0 | 16·0 | 24 | Drum |
| 44 | 38 | 34 | 76·6 | 18·2 | 24 | Drum |

Table 1. Computation time per time step and method of storage are shown for a wide range of resolutions

$\nu = 1{\cdot}008 \times 10^{-2}\,\text{cm}^2\,\text{sec}^{-1}$, $\kappa = 1{\cdot}420 \times 10^{-3}\,\text{cm}^2\,\text{sec}^{-1}$, $\beta = 2{\cdot}054 \times 10^{-4}\,(^{\circ}\text{C})^{-1}$. The Rossby and Taylor numbers are

$$\pi_4 \equiv (\beta g \Delta T d)/[\Omega^2(b-a)^2] = 0{\cdot}525 \quad \text{and} \quad \pi_5 \equiv 4\Omega^2(b-a)^5/(\nu^2 d) = 2{\cdot}041 \times 10^6$$

respectively. The computation was made with a resolution of $L = N = 33$ and $M = 37$ for a $\Phi = 2\pi$ sector to ascertain that wave-number 5 evolves. The calculation was repeated with $\Phi = 2\pi/5$ and the resulting steady-state solution is presented in figure 4.

The horizontal patterns of the pressure variable at the free surface, and in the Ekman layer on the base, are illustrated. Also shown are the vertical distributions of temperature and zonal velocity at the trough and ridge extremities of the surface wave pattern and similar distributions for the zonally averaged fields of temperature, zonal velocity and stream function $\psi$. The stream function for mean radial–vertical motion is defined as

$$r[v] = -\psi_z, \quad r[w] = \psi_r$$

where [ ] indicates zonally averaged variables.

The predominant features of the solution are (i) the formation of steady wave-number 5 which rotates in the direction of $\Omega$ (anticlockwise) at a rate of $\Omega/25$ rad/sec relative to the container; (ii) the triple cell system of the averaged meridional motion and (iii) the mainly positive flow of the zonal motion. Negative zonal velocities exist in the region of the base near the inner and outer cylinders; (iv) the different curvatures of the vertical temperature contours in the trough

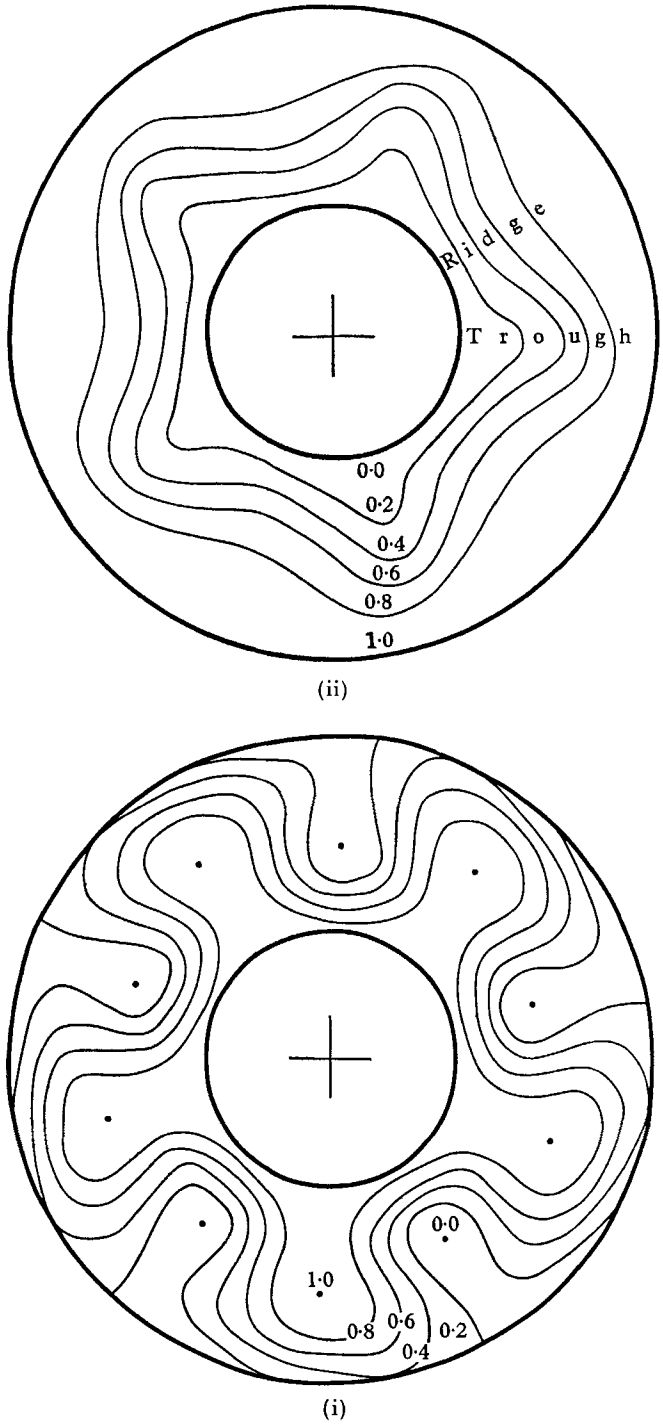


FIGURE 4(*a*). The horizontal distribution of pressure (i) in the Ekman layer near the bottom of the fluid ($z = \frac{1}{2}\Delta z$) and (ii) near the top of the fluid ($z = d - \frac{1}{2}\Delta z$). The absolute maximum and minimum pressure values are for (i) $-0{\cdot}3559$ and $-0{\cdot}6876$ cm$^2$ sec$^{-2}$ and for (ii) $1{\cdot}8174$ and $0{\cdot}6870$ cm$^2$ sec$^{-2}$. Note that the wave in the lower part of the fluid is 18° in front of the wave in the upper part. This phase difference is $\frac{1}{4}$ of a wavelength as in Eady's theory.

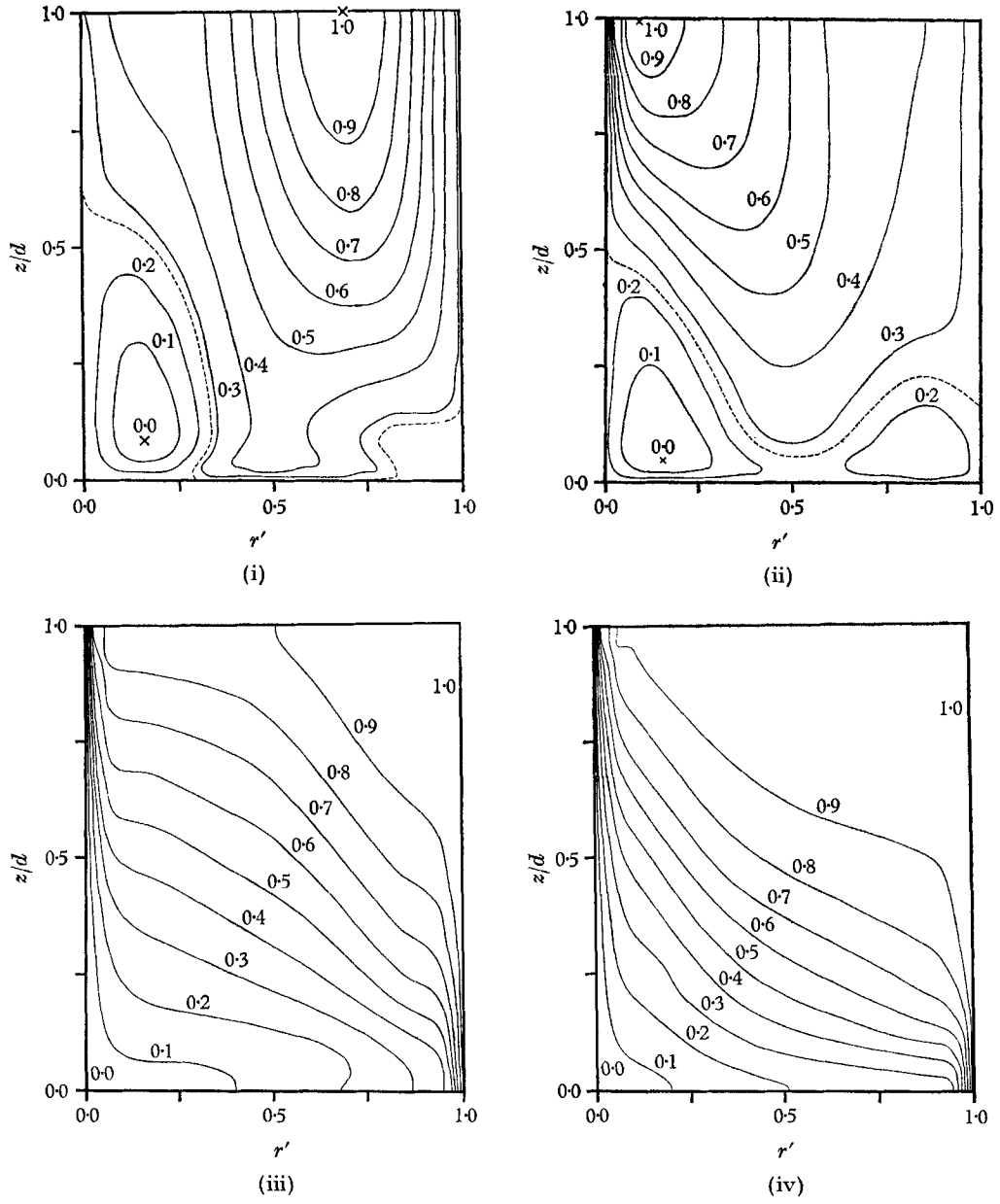


FIGURE 4(*b*). The steady-state contours of the vertical distribution of the zonal velocity at (i) the trough and (ii) the ridge and the temperature at (iii) the trough and (iv) the ridge of the surface wave. In all diagrams each variable is normalized with respect to its maximum and minimum values. The normalized maximum and minimum have the respective values of 1·0 and 0·0 and the other contours are at intervals of 0·1 (or 0·2 in figure 4(*a*)). The absolute value of a given contour of, e.g. $u$ may be determined from the relation $u = u\,\min + \text{contour value} \cdot \times \cdot (u\,\max - u\,\min)$. The absolute maximum and minimum values are 22·5, 17·5 °C for $T$ and 0·3522, −0·1321 cm sec$^{-1}$ for $u$ at the trough and 0·4601, −0·1573 cm sec$^{-1}$ for $u$ at the ridge. The broken line indicates the contour of zero zonal velocity above which the velocity is positive, i.e. in the same sense as the rotation, and below which it is negative. The non-dimensional radial co-ordinate $r' \equiv (r-a)/(b-a)$ commences at the cold inner cylinder (on the left of each diagram).

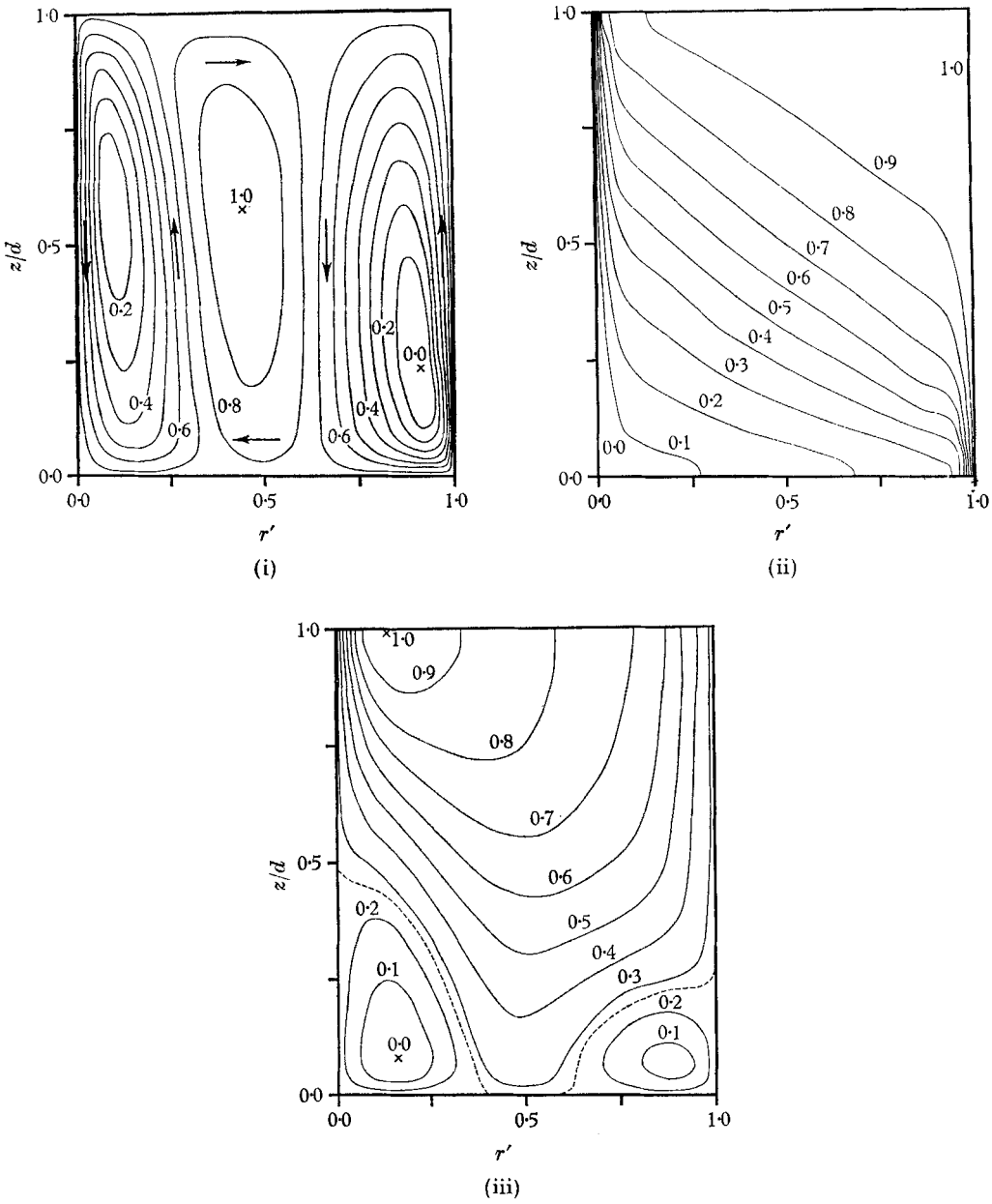


FIGURE 4(c). The steady-state contours of (i) stream function and zonally averaged (ii) temperature and (iii) zonal velocity. The absolute maximum and minimum values are 0·01759, −0·05347 cm³ sec⁻¹ for $\psi$, 22·5, 17·5 °C for $T$, and 0·3027, −0·1090 cm sec⁻¹ for $u$. The stream function arrows indicate the direction of the meridional flow.

and ridge and the linearity of the mean temperature field; (v) further analysis of the complete structure of the $T$, $p$ and $w$ waves to (be presented in the forthcoming paper) indicates phase and amplitude relationships similar to those of the classical Eady (1949) wave, suggesting that the wave flow is intrinsically a finite amplitude Eady wave.

The author wishes to acknowledge his indebtedness to Mr Henry Stambler for programming assistance. I am also grateful to Drs K. Bryan and K. Miyakoda for valuable suggestions and to M. B. Jackson and D. J. Johnson for preparing the figures.

## Appendix. Fast trigonometric transforms

A method for reducing the amount of computation time needed to perform the trigonometric analysis and synthesis in the solution of the Poisson equation will be presented. In recent years, methods of performing trigonometric transforms rapidly have been devised by Cooley & Tukey (1965) and Hockney (1965). The alternative method to be discussed here is a variation of the method of Danielson & Lanczos (1942). Only periodic analysis will be dealt with and the obvious extensions are left to the reader. The method avoids the restrictions and the logical complexity associated with the programming of the Cooley–Tukey method and for the range of harmonics normally used ($\leqslant 60$) is sufficiently rapid, affording an increase in speed of around 6·5 over the standard method of direct summation.

An analysis by periodic trigonometric series requires the multiplications and summations of the following type:†

$$\left.\begin{aligned} a_\alpha &= \sum_{s=0}^{4m-1} f_s . C_{\alpha s}, \quad \text{for} \quad \alpha = 0, 1, 2, \ldots, 2m; \\ b_\alpha &= \sum_{s=1}^{4m-1} f_s . S_{\alpha s}, \quad \text{for} \quad \alpha = 1, 2, \ldots, 2m-1, \end{aligned}\right\} \tag{A 1}$$

where

$$C_{\alpha s} = \Gamma_\alpha \left(\frac{1}{2m}\right)^{\frac{1}{2}} \cos\frac{\pi\alpha s}{2m}; \quad S_{\alpha s} = \left(\frac{1}{2m}\right)^{\frac{1}{2}} \sin\frac{\pi\alpha s}{2m}$$

for $s = 0, 1, 2, \ldots, 4m-1$ and $f_s$, the function being transformed is periodic so that $f_{4m} = f_0$. The method to be described allows the evaluation of $a_\alpha$, $b_\alpha$ with the amount of multiplication reduced by a factor of 8. As multiplication is a time-consuming operation this reduction is most useful. The number of grid intervals $M-1 = 4m$ has been chosen to be a multiple of 4 in order to derive the full benefit of the symmetry properties of the trigonometric functions in the four quadrants of the circle.

The reduction can be split up into three separate stages.

† For convenience the notation of § 6*b* is replaced by a simpler one.

(*a*) *Stage* 1. *Reduce the summation range from* $4m$ *to* $2m$

This is achieved by dividing the analysis into an even function (cosine) and odd function (sine) analysis by taking the sums and differences of the original ordinates. Thus, forming†

$$u_r = f_r + f_{4m-r}; \quad v_r = f_r - f_{4m-r} \quad \text{for} \quad r = 1, 2, \ldots, 2m-1 \tag{A 2}$$

and $u_0 = f_0$; $u_{2m} = f_{2m}$, and it can be shown by writing, e.g.

$$a_\alpha = \left( \sum_{s=0}^{2m} + \sum_{s=2m+1}^{4m-1} \right) f_s C_{\alpha s}$$

and simplifying the second integral, that

$$a_\alpha = \sum_{s=0}^{2m} u_s C_{\alpha s} \quad \text{for} \quad \alpha = 0, 1, \ldots, 2m, \tag{A 3}$$

$$b_\alpha = \sum_{s=1}^{2m-1} v_s S_{\alpha s} \quad \text{for} \quad \alpha = 1, 2, \ldots, 2m-1. \tag{A 4}$$

(*b*) *Stage* 2. *Reduce summation range from* $2m$ *to* $m$

Forming the sums and differences

$$\left.\begin{aligned} u''_r &= u_r + u_{2m-r} \\ u'_r &= u_r - u_{2m-r} \end{aligned}\right\} \quad \text{for} \quad r = 0, 1, \ldots, m-1,$$
$$\left.\begin{aligned} v'_r &= v_r + v_{2m-r} \\ v''_r &= v_r - v_{2m-r} \end{aligned}\right\} \quad \text{for} \quad r = 1, 2, \ldots, m-1, \tag{A 5}$$

and $u''_m = u_m$, $v'_m = v_m$, and then by splitting the summation range as in stage 1, we can show that

$$a_\alpha = \sum_{s=0}^{\left\{\begin{smallmatrix} m-1 \\ m \end{smallmatrix}\right\}} \begin{Bmatrix} u'_s \\ u''_s \end{Bmatrix} C_{\alpha s} \quad \text{for} \quad \alpha = \begin{Bmatrix} 1, 3, 5, \ldots, 2m-1 \\ 0, 2, 4, \ldots, 2m \end{Bmatrix}, \tag{A 6}$$

$$b_\alpha = \sum_{s=1}^{\left\{\begin{smallmatrix} m \\ m-1 \end{smallmatrix}\right\}} \begin{Bmatrix} v'_s \\ v''_s \end{Bmatrix} S_{\alpha s} \quad \text{for} \quad a = \begin{Bmatrix} 1, 3, 5, \ldots, 2m-1 \\ 2, 4, 6, \ldots, 2m-2 \end{Bmatrix}. \tag{A 7}$$

The numbers in the curly brackets are related by level. The double and single prime notation indicates variables with even and odd $\alpha$ values respectively.

(*c*) *Stage* 3. *Reduce the* $\alpha$ *range from* $2m$ *to* $m$

(This reduction of the summations (A 6) and (A 7) can be ignored if a gain of 4 rather than 8 is sufficient for the reader's purpose.)

The two coefficients $a_\alpha$ and $a_{2m-\alpha}$ contain two common series of alternate terms which differ only in sign. These series can be identified, defined and used to reduce the $\alpha$ range. Thus we can write:

$$\left.\begin{aligned} a_\alpha &= a'_\alpha + a''_\alpha, \\ a_{2m-\alpha} &= a''_\alpha - a'_\alpha, \end{aligned}\right\} \quad \text{for} \quad \alpha = 0, 1, 2, \ldots, m$$

and

$$\left.\begin{aligned} b_\alpha &= b'_\alpha + b''_\alpha, \\ b_{2m-\alpha} &= b'_\alpha - b''_\alpha, \end{aligned}\right\} \quad \text{for} \quad \alpha = 1, 2, 3, \ldots, m, \tag{A 8}$$

† The variables $u$, $v$, $r$ are separately defined to those in the main text.

$$\text{where}\quad \left.\begin{aligned} a'_\alpha &= \sum_{S_o}\begin{Bmatrix}u'_s\\u''_s\end{Bmatrix}C_{\alpha s}, & \begin{Bmatrix}S_o=1,3,5,\ldots,\text{mo}\\S_o=1,3,5,\ldots,\text{mox}\end{Bmatrix}&\begin{Bmatrix}\alpha=1,3,5,\ldots,\text{mox}\\\alpha=0,2,4,\ldots,\text{mex}\end{Bmatrix},\\ a''_\alpha &= \sum_{S_e}\begin{Bmatrix}u'_s\\u''_s\end{Bmatrix}C_{\alpha s}, & \begin{Bmatrix}S_e=0,2,4,\ldots,\text{me}\\S_e=0,2,4,\ldots,\text{mex}\end{Bmatrix}&\begin{Bmatrix}\alpha=1,3,5,\ldots,\text{mox}\\\alpha=0,2,4,\ldots,\text{mex}\end{Bmatrix},\\ b'_\alpha &= \sum_{S_o}\begin{Bmatrix}v'_s\\v''_s\end{Bmatrix}S_{\alpha s}, & \begin{Bmatrix}S_o=1,3,5,\ldots,\text{mox}\\S_o=1,3,5,\ldots,\text{mo}\end{Bmatrix}&\begin{Bmatrix}\alpha=1,3,5,\ldots,\text{mox}\\\alpha=2,4,6,\ldots,\text{mex}\end{Bmatrix},\\ b''_\alpha &= \sum_{S_e}\begin{Bmatrix}v'_s\\v''_s\end{Bmatrix}S_{\alpha s}, & \begin{Bmatrix}S_e=2,4,6,\ldots,\text{mex}\\S_e=2,4,6,\ldots,\text{me}\end{Bmatrix}&\begin{Bmatrix}\alpha=1,3,5,\ldots,\text{mox}\\\alpha=2,4,6,\ldots,\text{mex}\end{Bmatrix},\end{aligned}\right\} \tag{A 9}$$

where mox, mex are odd, even members of $(m, m-1)$ and mo, me are odd, even members of $(m-1, m-2)$ respectively, where double and single primes on $a_\alpha$, $b_\alpha$ indicate variables with even and odd $s$ values respectively.

To evaluate $a_\alpha$, $b_\alpha$ the summations (A 9) are used together with the folding functions defined in (A 8), (A 5) and (A 2). Although the number of multiplications needed to evaluate all the coefficients has been decreased by a factor of 8, the increased complexity of the summations reduces the net gain to 6·5.

## REFERENCES


ARAKAWA, A. 1966 Computational design for long term numerical integration of the equations of fluid motion. Two-dimensional incompressible flow. Part 1. *J. Comput. Phys.* **1**, 119.

BLACKMAN, R. B. & TUKEY, J. W. 1958 *The Measurement of Power Spectra.* New York: Dover.

BRYAN, K. 1966 A scheme for numerical integration of the equations of motion on an irregular grid free of non-linear instability. *Mon. Weath. Rev.* **94**, 39.

COOLEY, J. W. & TUKEY, J. W. 1965 An algorithm for the machine calculation of complex Fourier series. *Math. Comput.* **19**, 297.

DANIELSON, G. C. & LANCZOS, C. 1942 Some improvements in practical Fourier analysis and their application to X-ray scattering from liquids. *J. Franklin Inst.* **233**, 365.

EADY, E. T. 1949 Long waves and cyclone waves. *Tellus*, **1**, 33.

HAMMING, R. W. 1962 *Numerical Methods for Scientists and Engineers.* New York: McGraw Hill.

HARLOW, F. H. & WELCH, J. E. 1965 Numerical calculation of time dependent viscous incompressible flow of fluid with free surface. *Phys. Fluids*, **8**, 2182.

HENRICI, P. 1962 *Discrete Variable Methods in Ordinary Differential Equations.* New York: Wiley.

HOCKNEY, R. W. 1965 A fast direct solution of Poisson's equation using Fourier analysis. *J. Ass. Comput. Mach.* **12**, 95.

KURIHARA, Y. 1965 On the use of implicit and iterative methods for the time integration of the wave equation. *Mon. Weath. Rev.* **93**, 33.

LANCZOS, C. 1961 *Linear Differential Operators.* London: Van Nostrand.

LILLY, D. K. 1964 Numerical solutions for the shape preserving two-dimensional thermal convection element. *J. Atmos. Sci.* **21**, 83.

LILLY, D. K. 1965 On the computational stability of numerical solutions of time dependent non-linear geophysical fluid dynamics problems. *Mon. Weath. Rev.* **93**, 11.

MIYAKODA, K. 1962 Contribution to the numerical weather prediction: computation with finite difference. *Jap. J. Geophys.* **3**, 75.

PHILLIPS, N. A. 1959 An example of non-linear computational instability. *The Atmosphere and Sea in Motion.* New York: Rockefeller Inst. Press and Oxford University Press.

PLATZMAN, G. W. 1958 The lattice structure of the finite difference primitive and vorticity equations. *Mon. Weath. Rev.* **86**, 285.

RICHARDSON, L. F. 1922 *Weather Prediction by Numerical Process.* Cambridge University Press (Reprinted by Dover).

RICHTMYER, R. D. 1957 *Difference Methods for Initial Value Problems.* New York: Interscience.

SHUMAN, F. G. 1962 Numerical experiments with the primitive equations. *Proc. Int. Symp. on Numerical Weather Prediction.* Tokyo, 1960. Meteor. Soc. of Japan.

SMAGORINSKY, J. 1958 On the numerical integration of the primitive equations of motion for baroclinic flow in a closed region. *Mon. Weath. Rev.* **86**, 457.

SMAGORINSKY, J., MANABE, S. & HOLLOWAY, J. L. 1965 Numerical results from a nine-level general circulation model of the atmosphere. *Mon. Weath. Rev.* **93**, 727.

WILLIAMS, G. P. 1967 Thermal convection in a rotating fluid annulus, Parts I and II. *J. Atmos. Sci.* **24**, 144, 162.